BMC Cancer

RESEARCH

Open Access

# Neuropilin-1-target self-assembled peptide nanoparticles contribute to tumor treatment by inducing pyroptosis

Zheng Zhao[1†], Jingyun Wang[1†], Mengmeng Liu[2,3†], Ziqian Li[1], Fei Cao[1], Pengfei Xu[1], Qi Fang[1], Jie Yang[1], Zhulong Hu[1,4], Di Wu[1*], Rongbin Liu[5,6*] and Xuekui Liu[1*]

## Abstract

**Background** Expression of the Neuropilin-1 (NRP1) is reported in malignant cells of multiple human tumor types represented as a tumor marker. Targeting NRP1 with a peptide, CK3, is used for tumor molecular imaging, raising the question of the therapeutic potential of CK2, a peptide with a CK3 backbone which enhanced targeting and tumor enrichment properties.

**Methods** The tumor targeting and enrichment capacity of CK2 was detected by IncuCyte, flow cytometry and animal living imaging. To enhance its therapeutic efficacy, we developed a self-assembling peptide nanoparticles Fmoc-Gffy-AP-CK2, incorporating a peptide protective domain (Fmoc), a self-assemble domain (Gffy) and an anti-tumor peptide (AP). In vitro cellular assays and in vivo tumor-xenograft experiments were conducted to evaluate the anti-tumor effect of Fmoc-Gffy-AP-CK2.

**Results** While CK3 peptide specifically targets NRP1 in vitro and in vivo, CK2 markedly achieves stronger binding with NRP1 and higher tumor accumulation. Fmoc-Gffy-AP-CK2 exhibits a potent NRP1-dependent cytotoxic effect in vitro and in vivo. Mechanically, Fmoc-Gffy-AP-CK2 triggered caspase3/gasdermin E (GSDME)-mediated pyroptosis. Fmoc-Gffy-AP-CK2 also promotes the response rate of PD-1 checkpoint blockade.

**Conclusions** CK2, When combined with Fmoc-Gffy-AP domain, Demonstrated high anti-tumor efficacy, Providing a novel strategy for tumor treatment.

**Keywords** Neuropilin1, Cell-permeable peptides, Anti-tumor, Pyroptosis, Immunotherapy

†Zheng Zhao, Jingyun Wang and Mengmeng Liu contributed equally to this work.

*Correspondence:
Di Wu
wudi1@sysucc.org.cn
Rongbin Liu
liurb3@mail2.sysu.edu.cn
Xuekui Liu
liuxk@sysucc.org.cn
[1] State Key Laboratory of Oncology in South China, Guangdong Key Laboratory of Nasopharyngeal Carcinoma Diagnosis and Therapy, Guangdong Provincial Clinical Research Center for Cancer, Sun Yat-Sen University Cancer Center, 651 Dongfeng East Road, Guangzhou 510060, People's Republic of China
[2] Department of Oncology, The Second Affiliated Hospital JiangxiMedical College Nanchang University, Nanchang, China 330000
[3] Jiangxi Key Laboratory of Clinical Translational Cancer Research, Nanchang 330000, Jiangxi, China
[4] State Key Laboratory of Biocatalysis and Enzyme Engineering, School of Life Sciences, Hubei University, Wuhan 430062, China
[5] Department of Ultrasound, Sun Yat-Sen Memorial Hospital, Sun Yat-Sen University, Guangzhou 510120, China
[6] Guangdong Provincial Key Laboratory of Malignant Tumor Epigenetics and Gene Regulation, Sun Yat-Sen Memorial Hospital, Sun Yat-Sen University, Guangzhou 510120, China

## Background

The scientific advancements in our modern biological research greatly improve our understanding of malignant tumor. Small molecules, antibodies, short DNA aptamers and peptides are rational drug approaches [1, 2]. However, the majority group of druggable protein targets are only 3000 and our knowledge has not yet been adequate to find a cure for all cancers. Over the past decades, peptide drugs have increased significantly in the drug discovery landscape [3, 4]. Peptides exert their therapeutic effect through directly binding with their target or through conjugation to therapeutics, which are regarded as cargo for peptides [5, 6]. Thus, therapeutic peptides include cell-targeting peptides (CTP) and cell-permeable peptides (CPP) [7]. Rekdal et al. have reported that the position of a tryptophan residue, adjacent to the cationic region of a short amphipathic peptide and facilitated by the electrostatic interaction, aids in the insertion and subsequent cytotoxic activity of the peptide [8]. Such amphipathic bioactive peptides can also be used to drive "self-assembly" to form higher order peptide structures that can either be targeted directly to the membrane or can be guided through the membrane to attack intracellular targets upon assembly [9]. Over the past decades, Kuang et al. [10], Wang et al. [11] and Chen et al. [12] have tried to use self-assemble peptides to therapy cancer. The challenges to produce efficient and specific tumor-eradicating peptides not toxic to normal tissue are severalfold. Design a novel peptide-therapeutic complex, which can bind a molecular marker present on the targeted tumor cells and internalize to exert therapeutic effect while sparing other cells from the often toxin effect, is emergency for future cancer treatment.

Neuropilin-1 (NRP1) is single-pass transmembrane with a major role in immunity and tumorigenesis [13]. NRP1 is abundantly expressed within malignant cells of multiple human tumor types and tumor microenvironment, represented as a tumor therapeutic target [14, 15]. CK3, selected by phage display, was validated as a NRP1 targeting peptide and used for molecular imaging in breast cancer, which discovered by our lab [16, 17]. Qin et al. [18] had designed two probes on basis of the CK3 sequence, which achieved excellent specific targeting ability toward NRP1 and served as a platform for constructing dual-model or dual-targeting probes for tumor diagnosis. Conceivably, it's strikingly necessary to improve the affinity with NRP1 and boost the usages of CK3 to ameliorative clinical outcomes and favorable prognosis.

A successful example of therapeutic peptide was reported by Ellerby et al. [19]. They designed a pro-apoptotic peptide AP that was non-toxin outside cells, but toxin once internalizing into cells by disruption of mitochondrial membranes and activation caspase3 [19]. Peptide AP can't recognize target cells and internalize into cells itself [19]. CPP is need for AP to exerting its pro-apoptosis effect. Self-assembling L-peptide Gffy was applied to protect against peptide degradation and raise both humoral and cellular immune response [20, 21]. Moreover, short peptides modified with 9-fluorenylmethyloxycarbonyl (Fmoc) process excellent self-assembly capabilities and eminent application in drug delivery [22]. In this research, we modified CK3 to CK2 according that C-terminal arginine or lysine was essential to bind to NRP1 and penetrate cell membrane [17], which targeted more selectively to NRP1 and more accumulated in the tumor compared to other non-tumor bearing organs. Moreover, we incorporated the advances of AP, Gffy, Fmoc and CK2, and developed self-assembling peptide nanoparticles which specifically target NRP1-expression cancer cells (Scheme 1). This nanoparticle named Fmoc-Gffy-AP-CK2. We found Fmoc-Gffy-AP-CK2 were capable of cytotoxic and antitumor effect by activating caspase3/GSDME mediated pyroptosis. Importantly, Fmoc-Gffy-AP-CK2 also present a potent antitumor effect in subcutaneous mouse model with potent $CD8^+$ T cells stimulating property. Thus, Fmoc-Gffy-AP-CK2 may represent a novel and enticing approach for oncotherapy.

## Methods

### Peptide synthesis and labeling

AP-CK2, Fmoc-Gffy-CK2, Fmoc-Gffy-AP-CK2, Cy5-CK2 and Cy5-Ctrl were synthesized by Chinese Peptide Company (Hangzhou, China) using standard solid-phase Fmoc chemistry. Peptides were purified to a minimum purity of 95% high-performance liquid chromatography (HPLC), mass spectrometry (MS) and were isolated by lyophilization. The certificates of analysis were attached in supplementary files.

### Characterization

The electric potential and volume size distribution of Fmoc-Gffy-AP-CK2 nanoparticles were detected by dynamic light scattering (DLS) (Zetasizer Nano ZS, Malvern Instruments Limited, Malvern, Worcestershire, UK). Size and sharp of Fmoc-Gffy-AP-CK2 nanoparticles at nearly state were determined with a field emission scanning electron microscope (FESEM) by Novabio (China).

### Cell culture

S18, MDA-MB-231, A549, Capan2, KYSE450, LM3, HGC27, Hela and HCT116 were kindly provided by Dr. Musheng Zeng and cultured in complete RPMI 1640 (Sigma-Aldrich, #R8758-500 ml) with 10% Fetal Bovine Serum (FBS), 100U/ml penicillin/streptomycin (ThermoFisher, #15,140,122). The mice breast tumor cell

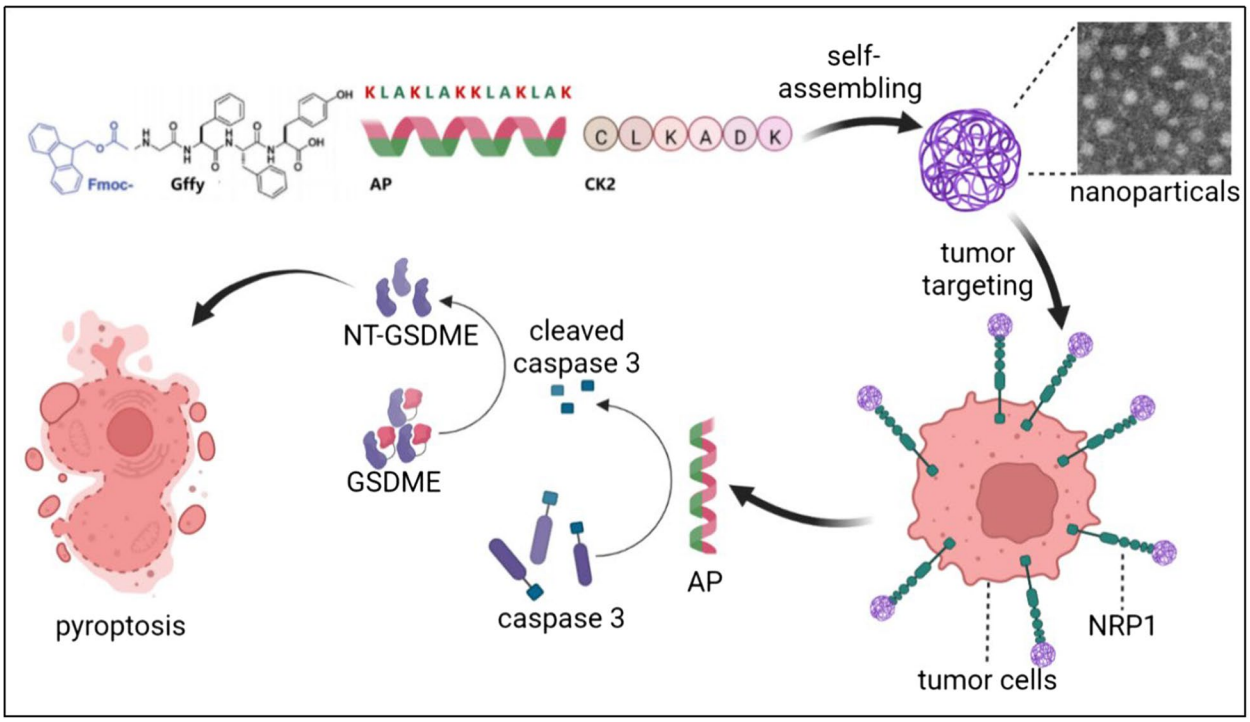


**Scheme 1** Schematic illuatration of the drug delivery and anti-tumor process of Fmoc-Gffy-AP-CK2. The self-assembling toxin nanocarrier Fmoc-Gffy-AP-CK2, that specifically targets NRP1, was designed to selectively deliver cytotoxic toxin AP to treat NRP1$^+$ tumor cells via activating caspase 3/GSDME pathways and triggering pytoptosis which boosted system immune

line 4T1 was cultured in complete Dulbecco's Modified Eagle's Medium (DMEM) (Sigma-Aldrich, #D6429-500 ml) and was also a gift of Dr. Zeng. All cells were incubated at 37℃ with 5% CO2 in a humidified atmosphere. All cell lines used in this study were authenticated using short tandem repeat (STR) profiling and regularly tested for mycoplasma contamination to ensure validity and reproducibility of the results.

### Cell viability assays

Cell viability upon AP-CK2, Fmoc-Gffy-CK2 and Fmoc-Gffy-AP-CK2 exposure was assessed with the Cell Counting Kit-8 (CCK8) (DOJINDO, #CK04) according to the manufacturer's instructions. Cells were seeded in 96-well plate (8000 cells/well) and treated with either buffer or different concentrations of AP-CK2 or Fmoc-Gffy-CK2 or Fmoc-Gffy-AP-CK2 (0–20 μM) for 60 min. CCK8 reagent was added into the plate and incubated at 37℃ for 4 h, and detected the absorbance.

### Clone formation

500 cells were added into each well of 6-well plate overnight. Cells were treated with different concentration of AP-CK2, Fmoc-Gffy-CK2 and Fmoc-Gffy-AP-CK2. The medium was refreshed every 4 days until clones could been observed by naked eye. After getting rid of the medium and washing by PBS, cells were fixed with 4% paraformaldehyde (Biosharp, #BL539A). Then 0.1% crystal violet (Macklin, #C805210) was used to stain clones after washing by PBS. Plate was washed under running water and air dried.

### Flow cytometry analysis

Cell viability upon AP-CK2, Fmoc-Gffy-CK2 and Fmoc-Gffy-AP-CK2 exposure was further assessed using the Annexin V-FITC/propidium iodide (PI) Kit (KeyGEN, #KGA108) according to the manufacturer's instructions. 30,000 cells were plated in per well of 6-well plate and exposed to 1.5 μM, 3 μM or 6 μM of AP-CK2, Fmoc-Gffy-CK2 or Fmoc-Gffy-AP-CK2 for 60 min. Cells were collected and analyzed by CytoFLEX LX (Beckman Coulter).

### LDH release assay

LDH release from S18 and MDA-MB-231 cells upon AP-CK2, Fmoc-Gffy-CK2 and Fmoc-Gffy-AP-CK2 exposure was studied using LDH Cytotoxicity Assay Kit (Beyotime, #C0017). Cells were seeded in 96-well plate and added assay reagents after 24 h treatment according to the manufacturer's instructions.The absorbance at 490 nm was measured by a multi-well apectrophotometer (Bio-Tek EPOCH).

### Western blotting

Protein was extracted by RIPA and quantified by BCA protein assay kit (ThermoFisher, #23,225). Protein samples were boiled in 5×SDS PAGE loading buffer for 5 min and loaded to 10% SDS PAGE gels for protein separation. Protein was transferred to polyvinylidene fluoride (PVDF) membrane (Merck millipore, #ISEQ00010) and membrane was blocked in 5% non-fat milk for 60 min at room temperature with gentle shaking. The primary antibodies were used to incubate with membrane at 4℃ overnight. Followed by washing with PBST for 3 times, the membrane was incubated with the HRP-conjugated secondary antibodied for 60 min at room temperature. Finally, membranes were visualized by enhanced chemiluminescence (ECL) (Zen BioScience, #17,046-500 ml) and imaged with Tanon 5200 Multi instrument (Shanghai, China) as recommended by the manufacturer.

### In vivo *experiments*

Five-week-old female nude BALB/c mice and BALB/c mice were purchased from Charles River (Zhejiang, China) and housed in a specific pathogen-free (SPF) environment with sterile food and water. All animal experiments were proved by the ethics committee of Sun Yat-sen University (approval No. L025503202205014).

To detect the biodistribution of CK2 peptide were labelled with the fluorescence dye Cy5 using Cy5 label kit (Ginbio, #GB70010) according to the instructions of the manufacturer. BALB/c bearing MDA-MB-231 xenografts were intravenously injected with 20 nmol Cy5-labelled peptides in 100 μl PBS for 24 h. The biodistribution of Cy5 were analyzed by bioluminescence imaging using IVIS Spectrum (Xenogen) and then the mice were euthanized. Organs were collected and quantitative imaging immediately.

To assess Fmoc-Gffy-AP-CK2 cytotoxic effect, animals bearing Hela tumors of approximately 100 $mm^3$ were randmized into 4 groups ($n=5$ per group). 1 mg of AP-CK2, Fmoc-Gffy-CK2, Fmoc-Gffy-AP-CK2 or buffer were intravenously administered to the animals every other day. Tumor size and body weight were measured three times per week with the caliper (tumor volume = width × width × length/2). After 30 days, animals were euthanized using carbon dioxide ($CO_2$) asphyxiation in a chamber designed for small laboratory animals. Tumor tissues and other organs were collected and fixed into formalin/RNA later buffer (ThermoFisher, #AM7021) for further analysis.

To investigate the immune effect in vivo, $1\times10^6$ 4T1 cells were subcutaneous injected into the back of BALC/c mice. When the volume grew to 100 $mm^3$, PD-1 antibody and Fmoc-Gffy-AP-CK2 were used in mice. Fmoc-Gffy-AP-CK2 administration approach was intravenous injection and PD-1 antibody was intraperitoneal injection: group one, 100 μl PBS; group two, Fmoc-Gffy-AP-CK2 with the dose of 100 μg/100 μl; group three, PD-1 antibody with the dose of 200 μg/100 μl; group four, 100 μg Fmoc-Gffy-AP-CK2 and 200 μg PD-1 antibody in 100 μl. After 30 days, animals were euthanized using carbon dioxide ($CO_2$) asphyxiation in a chamber designed for small laboratory animals. Tumor tissues and other organs were collected and fixed into formalin/RNA later buffer (ThermoFisher, #AM7021) for further analysis.

### Histological analysis

Tissues from mice were fixed in 4% paraformaldehyde and embedding with paraffine. 4 μm sections were cut by Leica Microtome and examined by hematoxylin and eosin (BASMEDTSCI, #BP0211) staining. For immunohistochemical (IHC) analysis, tissue sections were deparaffinized, hydrated and retried antigen in citrate-based unmasking solution (ZSGB-BIO, #ZLI-9065) by heating in autoclave cooker for 10 min. Sections were washed in PBST (PBS with 0.1% Tween-20) and blocked in normal goat serum (CoWin Biosciences, #CW0130S) for 1 h. Slides were incubated overnight at 4 ℃ in a humidified chamber with the following primary antibodies: anti-N-GSDME (Abcam, #ab222407), anti-cleaved-caspase 3 (Abcam, #ab32042), anti-Ki67 (Proteintech, #27,309–1-AP). After washing, secondary antibody HRP-conjugated goat anti-rabbit antibody (ThermoFisher, #31,460) was applied for 1 h at room temperature. Slides were stained with hematoxylin and mounted with neutral resins (Splarbio, #G8590).

### Statistical analysis

All experiment were performed in triplicate. Data were showed as mean ± SD. GraphPad Prism 8 sofware (GraphPad Sofware, San Diegom, California USA) was used for statistical analyses. Differences between groups with Gaussian distribution were analyzed by using t-test, otherwise Wilcoxon rank sum test was used. Values of $p<0.05$ were considered statistically significant.

## Results

### CK2 achieves a strong binding with NRP1 and high tumor accumulation in subcutaneous tumor model

In the previous study, a specific NRP1 targeting peptide CK3 (CLKADKAKC) was screened by phage display and the function was verified in vitro and in vivo [16]. Subsequently, based on CK3, a peptide CK2 (CLKADK) with theoretically stronger binding ability was designed. We have found that compared with CK3, the optimized CK2 achieved a higher affinity with NRP1 in vitro [23].

To investigate whether NRP1-targeted peptide CK2 could be targeted NRP1-expression tumor or not,

Cy5-labeled CK2 (CK2-Cy5) were intravenously injected into mice model bearing MDA-MB-231 subcutaneous tumor. The fluorescence imaging was captured by IVIS Spectrum. Cy5 fluorescence was used as a negative control. Whole-body fluorescence imaging revealed that Cy5-labeled CK2 specifically accumulated in subcutaneous and a small accumulation in the kidney (Fig. 1A). Furthermore, mouse tissues imaging showed that Cy5-labeled-CK2 was enriched in the tumor and excreted in the kidney 24 h after injection (Fig. 1B and C). Then we

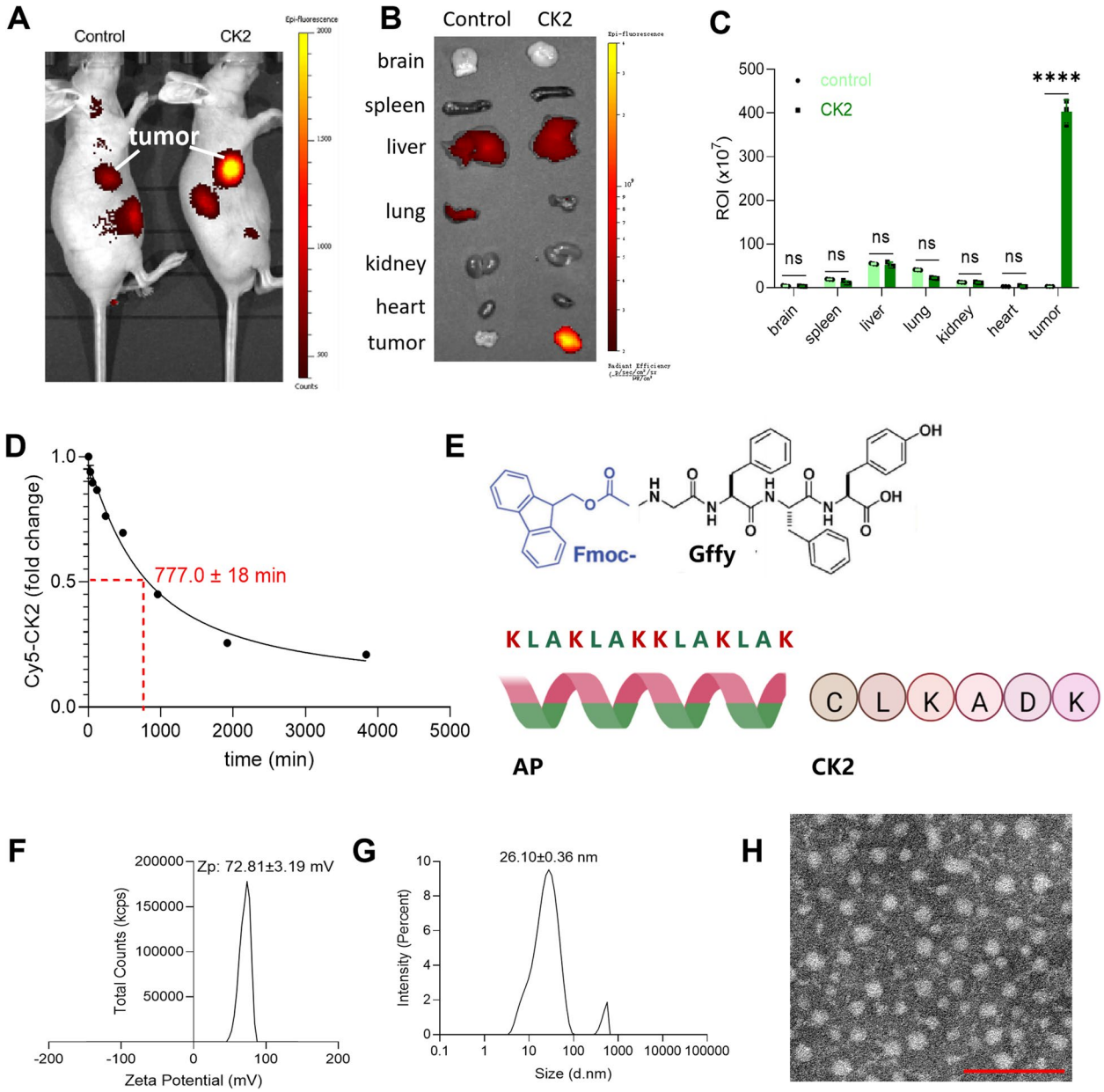


**Fig. 1** NRP1-target peptide CK2 accumulated in tumor and Fmoc-Gffy-AP-CK2 nanoarchitecture were characteristic. **A** In vivo tumor homing of Cy5-labeled CK2. Mice bearing MDA-MB-231 tumors were intravenously injected with 200 μg of Cy5-labeled CK2 or Cy5-labeled control peptide. Near-infrared fluorescence (NIRF) imaging was performed 12 h post-injection to visualize tumor accumulation. **B** Fluorescence in excised organs was measured to evaluate tissue distribution of Cy5-labeled CK2 and control peptide. **C** 0.1 μg Cy5-CK2 was mixed with 30 μL of mice sera and incubated at 37 °C for different durations as indicated, the degradation of Cy5-CK2 was evaluated by flow cytometry assays, and the degradation curve was drawn using nonlinear regression based on fluorescence value. **D** The region of interest (ROI) in (B)was represented as the max radiant efficiency. **E** Fmoc-Gffy-AP-CK2 is divided in four fragments. **F** Z-potential (Zp) values of Fmoc-Gffy-AP-CK2 were determined to evaluate surface charge. **G** Size of Fmoc-Gffy-AP-CK2 nanoparticles was measured by DLS. **H** FESEM image of Fmoc-Gffy-AP-CK2 showed nanoparticle structure. Bars indicate 100 nm

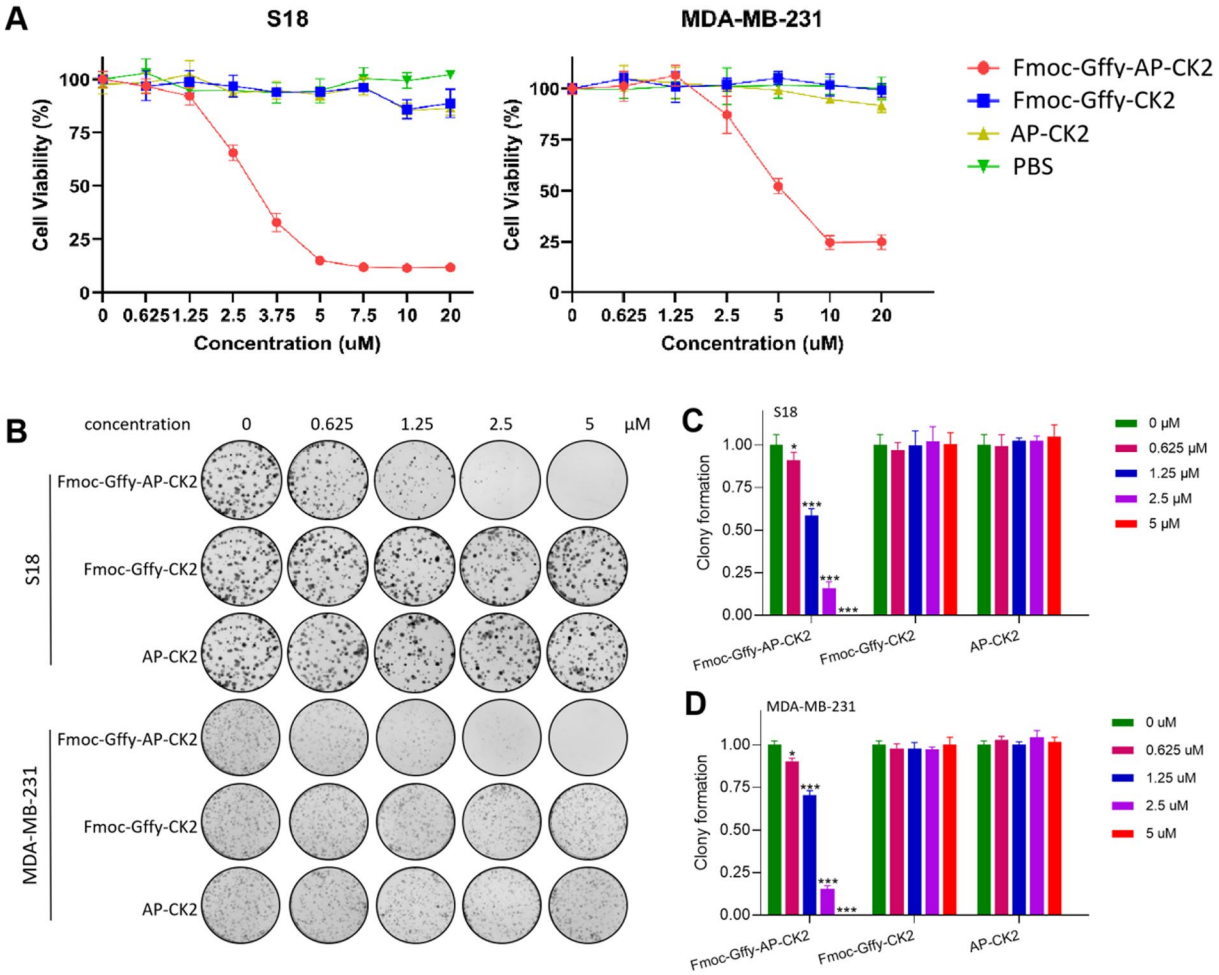


**Fig. 2** Fmoc-Gffy-AP-CK2 cytotoxic effect in tumor cell lines. **A** Dose-dependent cytotoxic effects of AP-CK2, Fmoc-Gffy-CK2, and Fmoc-Gffy-AP-CK2 (0–20 μM) on S18 and MDA-MB-231 cell lines after 1 h of exposure. Cell viability was assessed, and $IC_{50}$ values were determined for each compound. **B** Colony formation assay experiments were performed for S18 and MDA-MB-231 with AP-CK2, Fmoc-Gffy-CK2 or Fmoc-Gffy-AP-CK2 treatment. Representative images of S18 (up) and MDA-MB-231(down) colony formation after treatment were shown. **C** and **D** Mean colony numbers were measured after treatment and the results of S18 (**C**) and MDA-MB-231 (**D**) were presented as Mean ± S.D.. ***$p < 0.005$

incubated Cy5-CK2 in mice serum samples at 37℃ for different times, and the results showed that the half-life of Cy5-CK2 in sera from mice was 12.95 ± 0.3 h (Fig. 1D). Taken together, these data indicated that NRP1 is the cellular target of CK2 and CK2 achieved strong biomacromolecules uptake efficiency in vivo.

### *CK2 self-assembled nanoparticles induce anti-tumor effect* in vitro

Peptide AP, first repored by Ellerby et al., is a cationic peptide with α helical structure which could destroy mitochondria membrane, release cytochrome C and active caspase3 [19]. But without CPP, AP can't enter cells. Peptide Gffy could be coupled with peptides to form nanospheres and increase the stability of peptides [20,

**Table 1** $IC_{50}$ values of Fmoc-Gffy-AP-CK2 treatment in tumor cell lines

| tumor | Cell lines | $IC_{50}$ |
|---|---|---|
| Nasopharyngeal tumor | S18 | 2.88 |
| Breast tumor | MDA-MB-231 | 4.05 |
| | 4T1 | 10.07 |
| Lung tumor | A549 | 9.17 |
| Esophageal tumor | KYSE450 | 15.87 |
| Pancreatic tumor | Capan-2 | 8.12 |
| Liver tumor | LM3 | 7.32 |
| Stomach tumor | HGC27 | 5.94 |
| Colorectal tumor | HCT116 | 9.8 |

$IC_{50}$ values show the Fmoc-Gffy-AP-CK2 concentration (μM) (concentration, mean (95% confidence intervals))

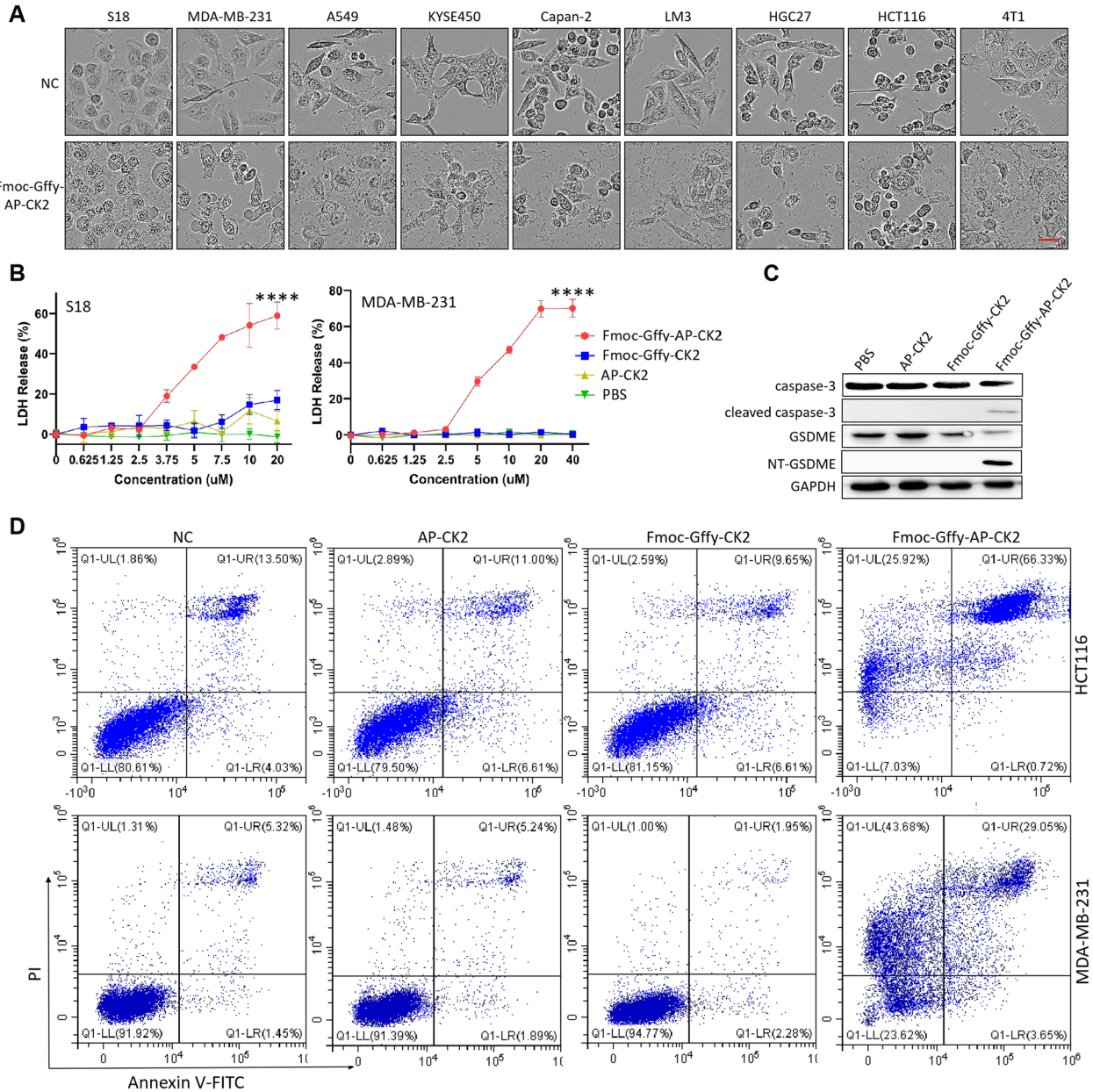


**Fig. 3** Fmoc-Gffy-AP-CK2 activated caspase3/GSDME-mediated pyropsosis. **A** Representative images of tumor cells treated with or without Fmoc-Gffy-AP-CK2 for 1 h. Pyroptotic morphological changes, including cell swelling and membrane rupture, were observed at 200× magnification. **B** Quantification of LDH release as an indicator of membrane disruption in S18 and MDA-MB-231 cells treated with AP-CK2, Fmoc-Gffy-CK2, or Fmoc-Gffy-AP-CK2 at various concentrations. ***$p < 0.0001$. **C** Representative images of pro-caspase3, cleaved-caspase3, GSDME, NT-GSDME and GAPDH western blots of samples from MDA-MB-231 cell lines exposed to AP-CK2, Fmoc-Gffy-CK2 or Fmoc-Gffy-AP-CK2 for 1 h. **D** Cell viability of HCT116 and MDA-MB-231 cells either treated with AP-CK2, Fmoc-Gffy-CK2 or Fmoc-Gffy-AP-CK2

(See figure on next page.)

**Fig. 4** In vivo antitumor effect of Fmoc-Gffy-AP-CK2. **A** Antitumor efficacy of Fmoc-Gffy-AP-CK2 on Hela tumor-bearing nude mice in vivo ($n = 5$ biologically independent mice per group). Schematic illustration the treatment schedule of AP-CK2, Fmoc-Gffy-CK2 or Fmoc-Gffy-AP-CK2 against cervical tumor. **B** Tumor size was measured over 13 days, showing growth trends for each mouse in the treatment groups. **C** Quantitative results of tumor weight excised at the end of the antitumor studies. **D** Tumors were harvested at day 13 to visually compare sizes across treatment groups. **E** Representative IHC images of tumor sections stained for Ki-67 and cleaved caspase-3. Scale bar in green, 100 μm. Scale bar in black, 50 μm. **F** Positive tumor cells from random fields of each image were normalized against total tumor cells stained by hematoxylin

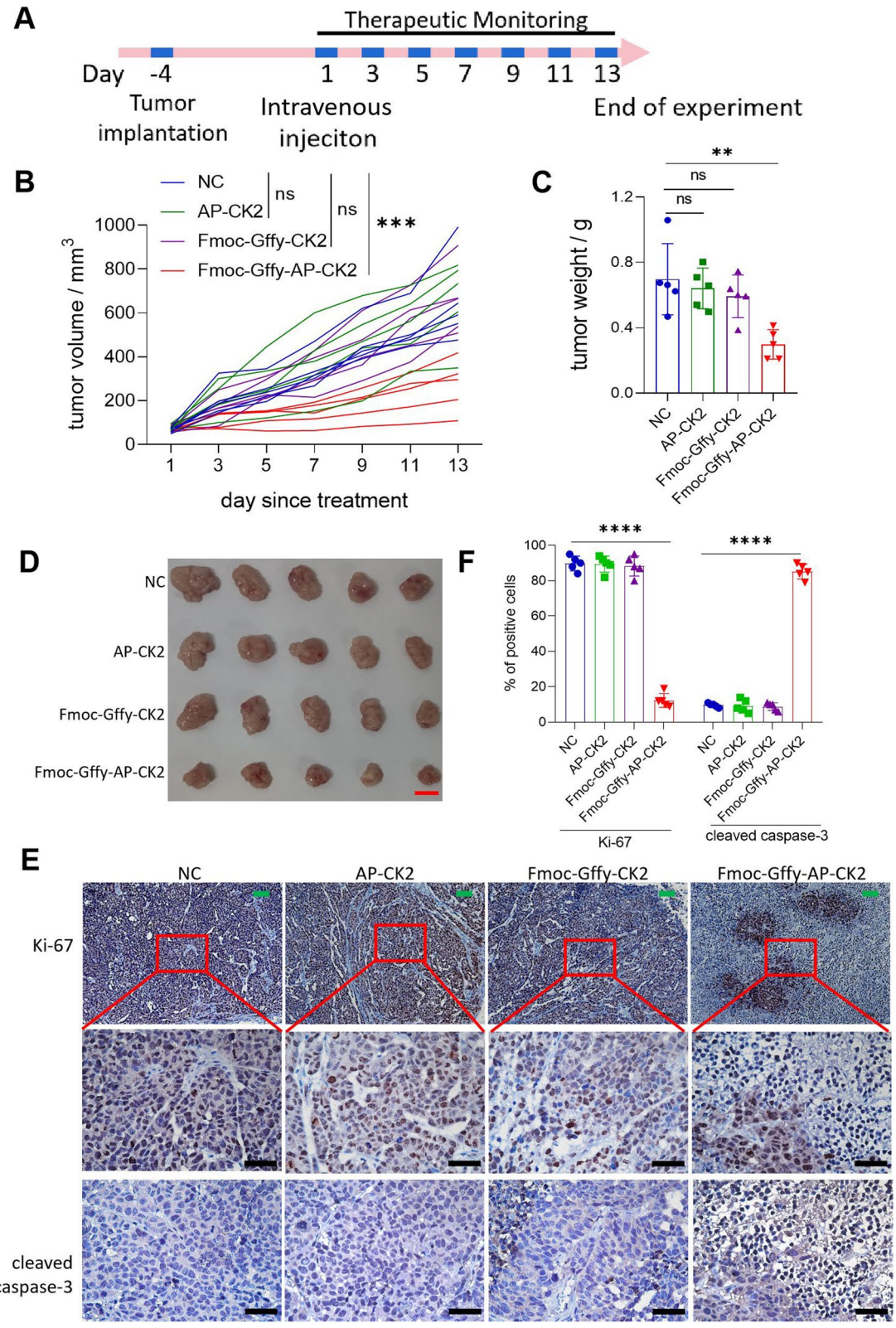


**Fig. 4** (See legend on previous page.)

21]. In addition, the self-assembly of anti-tumor peptides form a slow-release system targeting the tumor microenvironment. Fmoc is a protective group which protect peptides from acids [22]. Base on NRP1 targeting peptide CK2, we combined peptide Fmoc, Gffy, AP and CK2 to design an anti-tumor self-assembled nanoparticles Fmoc-Gffy-AP-CK2 (Fig. 1E). AP-CK2 and Fmoc-Gffy-CK2 were designed as a negative control. Fmoc-Gffy-AP-CK2 nanoparticles, with positive potential 72.81 ± 3.19 mV (Fig. 1F), self-assemble into ~ 20 nm (Fig. 1G). The assembled proteins appeared as toroid materials, with ultrastructural morphometry (round shape and clear size populations) that confirmed the size range observed by dynamic light scattering (DLS) (Fig. 1H).

To determine if Fmoc-Gffy-AP-CK2 treatment would kill tumor cells, the cytotoxicity of AP-CK2, Fmoc-Gffy-CK2 and Fmoc-Gffy-AP-CK2 were detected by CCK8. Surprisingly, AP-CK2 and Fmoc-Gffy-CK2 did not show any cytotoxic effect on tumor cells while all tumor cell lines showed different cell death in response to Fmoc-Gffy-AP-CK2 (0.625–20 μM) (Fig. 2A, Figure S1 and Table 1). Thus, Fmoc-Gffy-AP-CK2 exposure induced cell death in nasopharyngeal tumor, breast tumor, lung tumor, esophagus tumor, pancreatic tumor, liver tumor, stomach tumor and colorectal tumor cell lines.

### CK2 self-assembled peptide nanoparticles inhibit tumor cell proliferation

To address the effect of Fmoc-Gffy-AP-CK2 on tumor cell proliferation, we assessed the clone formation in S18 and MDA-MB-231 cell lines exposing to AP-CK2, Fmoc-Gffy-CK2 and Fmoc-Gffy-AP-CK2. We clearly observed decreased clone formation with Fmoc-Gffy-AP-CK2 treatment by concentration dependent pathway (Fig. 2B-D). Thus, Fmoc-Gffy-AP-CK2 might be a neotype tumor-target cytotoxic agent.

### CK2 self-assembled peptide nanoparticles activate caspase3/GSDME-mediated pyroptosis in tumor cells

The ability of Fmoc-Gffy-AP-CK2 to treat tumor cells in vitro prompted us to ask the molecular mechanism of Fmoc-Gffy-AP-CK2 in anti-tumor. Intuitively, bubbles were forming on the surface of the cell within the treatment of Fmoc-Gffy-AP-CK2 (Fig. 3A). Assuredly, we inferred that Fmoc-Gffy-AP-CK2 induced tumor cell death by pyroptosis. Then we detected that the percentage of LDH release in the cells after treatment of AP-CK2, Fmoc-Gffy-CK2 and Fmoc-Gffy-AP-CK2. As expected, Fmoc-Gffy-AP-CK2 treatment promoted LDH release (Fig. 3B). In addition, we detected the activation of caspase3 and the cleaved situation of GSDME by western blot. Results indicated that Fmoc-Gffy-AP-CK2 activated caspase3 and then cleaved GSDME, resulting in pyroptosis of tumor cells (Fig. 3C and Figure S2). Finally, Annexin V/PI assay also showed cell pyroptosis with Fmoc-Gffy-AP-CK2 treatment (Fig. 3D). These results suggest that Fmoc-Gffy-AP-CK2 treatment may lead to tumor cell pyroptosis, contributing to tumor treatment.

### *CK2 self-assembled peptide nanoparticles inhibit tumor growth* in vivo

Owing to the excellent performance of Fmoc-Gffy-AP-CK2 in the cellular research, nude BALB/c mice were used to investigated its antitumor effect in vivo. Following establishment of the AP-CK2, Fmoc-Gffy-CK2 or Fmoc-Gffy-AP-CK2 treatment model, mice were treated with AP-CK2, Fmoc-Gffy-CK2 or Fmoc-Gffy-AP-CK2 (100 μg/mouse, i.v.) on the other days after tumor grown to 100 $mm^3$ (Fig. 4A). Fmoc-Gffy-AP-CK2 treatment resulted in reduction of tumor burden compared with PBS, AP-CK2 or Fmoc-Gffy-CK2 treatment (Fig. 4B-D). Moreover, Ki-67 and cleaved caspase-3 staining showed that Fmoc-Gffy-AP-CK2 treatment significantly inhibited the proliferation of tumor cells and reduced the number of tumor cells (Fig. 4E and F). The cleaved caspase-3 staining also indicated that Fmoc-Gffy-AP-CK2 might kill tumor cells by pyroptosis in vivo. The H&E staining revealed that the high selectivity of Fmoc-Gffy-AP-CK2 towards cancer cells caused extensive tumor cell killing with reduced toxity towards surrounding healthy tissues (Figure S3).

Accumulating evidence shows that pyroptosis triggers the inflammatory tumor microenvironment and enhances the efficacy of cancer immunotherapy [24, 25]. Given the high efficiency of Fmoc-Gffy-AP-CK2-mediated pyroptosis, we exploited these nanoparticles combined with PD-1 antibody for cancer therapy (Fig. 5A). Results showed that Fmoc-Gffy-AP-CK2 combined with

(See figure on next page.)

**Fig. 5** Immune response in vivo. **A** A schematic illustration of the treatment schedule for Fmoc-Gffy-AP-CK2 and/or PD-1 antibody administration in the breast tumor model. **B** Graph showing individual tumor growth curves ($n = 5$ for each therapeutic group) over a period of 13 days after the initiation of the treatment (day 1). ns: not significant; ***: $p < 0.001$. **C** Representative images of excised tumors from each treatment group at the end of the study. D Quantification of tumor weights in the 4T1 breast tumor model following treatment ($n = 5$ per group), demonstrating significant differences between groups. ns: not significant; **: $p < 0.01$; ***: $p < 0.001$. **E** Immunofluorescence analysis showing the proportion of tumor infiltrating $CD3^+$ (green) and $CD8.^+$ (red) T cells. (Magnification 100×)

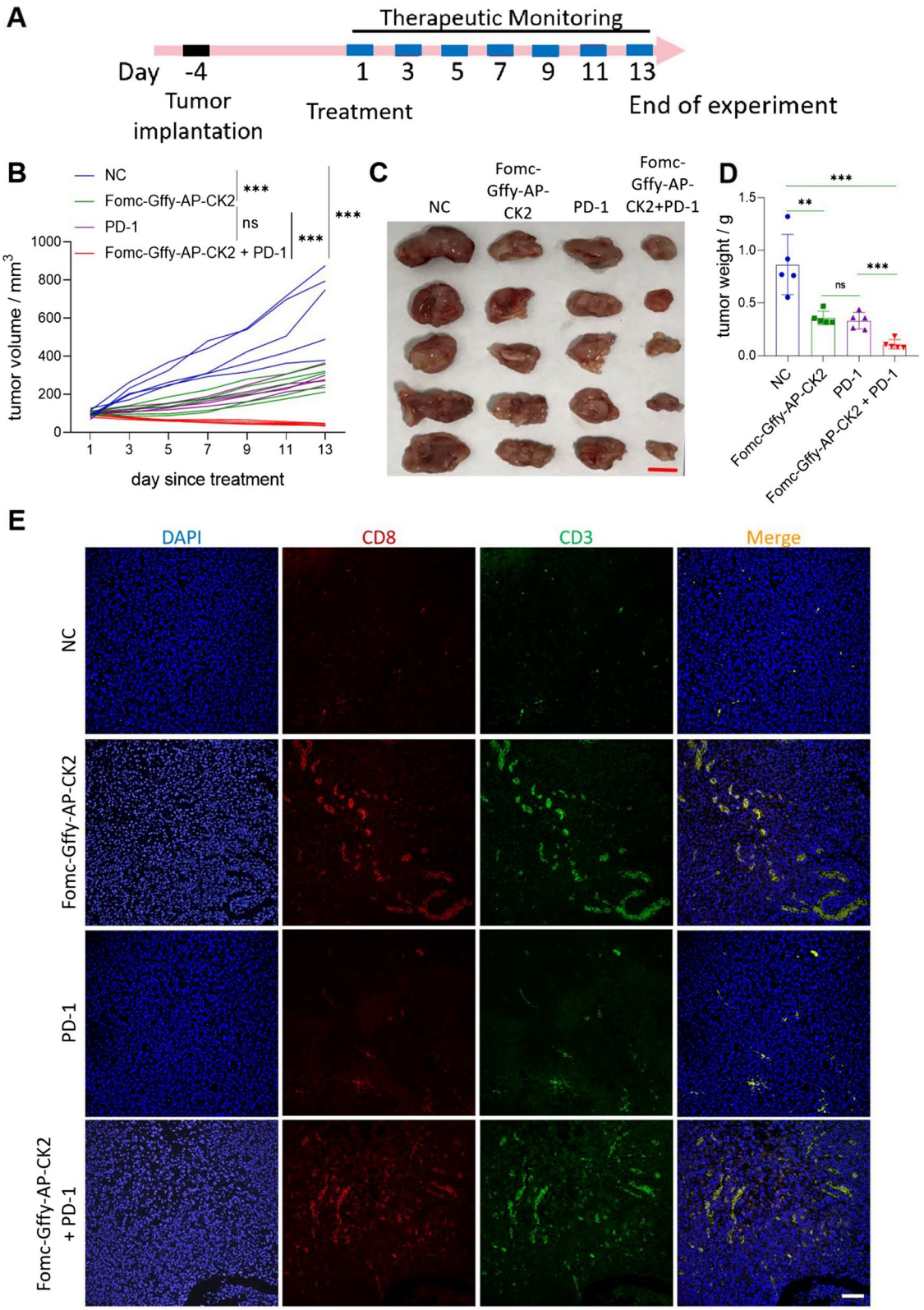


**Fig. 5** (See legend on previous page.)

PD-1 antibody therapy almost removed the 4T1 tumor (Fig. 5B and Figure S4A). Compared with PD-1 antibody, the efficacy of Fmoc-Gffy-AP-CK2 + PD-1 antibody was dramatically compromised in the tumor models (Fig. 5C-D) without obviously body weight change (Figure S4B). The Fmoc-Gffy-AP-CK2 treatment promoted the number and function of tumor-infiltrating $CD3^+$ and $CD8^+$ T cells (Fig. 5E). Neither did we observe any changes in other organs (Figure S4C). Therefore, Fmoc-Gffy-AP-CK2 elicited systemic antitumor immune response with no side effects due to highly NRP1 specific.

## Discussion

The systemically administered chemotherapy for cancers exploits the cytotoxic activities of drugs. However, the lack of drug targeting induces severe side effects limiting the usable drug concentration, which remains insufficient to prevent cancer proliferation, recurrence and metastasis [26–28]. Tumor-target drugs are concomitantly urge to enhance life quality and survival expectancy. A growing body of relevant evidence suggests that the expression of NRP1 has inevitably links it to cancer [29–31]. Studies have indicated that NRP1 is up-regulated in cancers at mRNA and protein levels [32, 33]. Likewise, the stimulated expression of NRP1 on the surface of cancer cells were conducted to test NRP1 as a therapeutic target. Our lab has been reported NRP1-targeting peptide identification of CK3 [16]. The CK3 peptide is well binding with NRP1 and showed an accumulating activity to cancer without other organs congestion, except for the metabolic kidney. For cancer chemotherapy, CK3 is still need to promote selective uptake of attached cargos. In this study, we identified that CK2, a shorter amino acid segment of CK3, is a stronger peptide for extracellular targeting in $NRP1^+$ cells. The selectivity, stability and efficacy of CK2 have been fully demonstrated in vitro and in vivo, which were more outstanding than CK3 [23].

AP is a short peptide composed of tumor blood vessel "homing" motif and a programmed cell death-triggering sequence [19]. However, the targeting tumor cells and internalization activities of AP were limiting its usage. If such powerful pro-apoptotic peptide were coupled to a more powerful tumor targeting peptide that allow receptor-mediated internalization, the chimeric peptide may yield new cancer therapy agents. Thus, we designed NRP1-target self-assembled peptide nanoparticles composed self-assembling domain Gffy and Fmoc, toxic domain AP, and tumor-targeting domain CK2. Nanoparticles is optimal to promote the rate of uptake and intercellular concentration on certain mammalian cells [34, 35]. Our experiments firstly demonstrated that Fmoc-Gffy-AP-CK2 could effectively induce pyroptosis, while western blotting studies revealed a mechanism of action involving a caspase3/GSDME signaling pathway. In addition, we note that Fmoc-Gffy-AP-CK2 displayed excellent anti-tumor efficacy, as well as an ability to enhance immune response. IHC analyses of tumor tissues from Fmoc-Gffy-AP-CK2 treated mice demonstrated significant upregulation of cleaved caspase-3, providing evidence of peptide-induced pyroptosis in vivo. The toxicity of Fmoc-Gffy-AP-CK2 towards normal tissues almost could not be detected. However, the potential long-term toxicity, safe and biodegradation of our Fmoc-Gffy-AP-CK2 needs to be comprehensively evaluated for further biomedical applications.

At present, we only detected the half-life of CK2 in sera from mice. More detailed pharmacokinetic data need to be characterized. While the study employs cell cultures to investigate the interaction between Fmoc-Gffy-AP-CK2 and the mice immune system, these models might not fully replicate the complexity of human immune response. Translating these findings into effective therapies presents significant challenges. The development of therapeutic agents targeting NPR1 or the caspase3/GSDME pathway requires careful consideration of safety, specificity, and efficacy.

## Conclusions

The peptide CK2, a ligand of NRP1, has been shown to be a powerful tag for targeting in NRP1 + cells, both in cultured cells and in vivo. CK2 is able to fuse Fmoc, Gffy and AP as self-assembling nanoparticles (26 nm in mean diameter) for cancer therapy. Fmoc-Gffy-AP-CK2 enhanced tumor immunotherapy by trigger cancer cell pyroptosis. Our experiments also indicate that Fmoc-Gffy-AP-CK2 may effectively focus on caspase3/GSMDE to promote pyroptosis and evoke immune response. More interestingly, Fmoc-Gffy-AP-CK2 therapy achieves an effective inhibition on tumor growth combining with PD-1 antibody therapy, which could become a new strategy for improving anti-tumor immune response.

### Abbreviations

| | |
|---|---|
| CCK8 | Cell Counting Kit-8 |
| CPP | Cell-permeable peptides |
| CTP | Cell-targeting peptides |
| DLS | Dynamic light scattering |
| DMEM | Dulbecco's Modified Eagle's Medium |
| ECL | Enhanced chemiluminescence |
| FBS | Fetal Bovine Serum |
| Fmoc | 9-Fluorenylmethyloxycarbonyl |
| HPLC | High-performance liquid chromatography |
| IHC | Immunohistochemical |
| MS | Mass spectrometry |
| NRP1 | Neuropilin-1 |
| PVDF | Polyvinylidene fluoride |
| SPF | Specific pathogen-free |
| STR | Short tandem repeat |

## Supplementary Information

The online version contains supplementary material available at https://doi.org/10.1186/s12885-025-13784-y.

Supplementary Material 1.

**Acknowledgements**
Not applicable.

**Authors' contributions**
Conceptualization, X.L., R.L., D.W. and Z.Z.; methodology, Z.Z., J.W. M.L. and Z.L.; validation, Z.Z., J.W. and Z.L.; investigation, Z.Z., J.W., M.L., Z.L., S.L, F.C., P.X., Q.F., J.Y. and Z.H.; data curation, Z.L. and Z.H.; writing—original draft preparation, Z.Z. M.L., and Z.L.; writing—review and editing, Z.Z., J.W. and Z.L.; visualization, Z.Z., J.W and Z.L.; supervision, X.L., R.L. and D.W.; project administration, X.L., R.L., D.W., Z.Z. and Z.L.; funding acquisition, R.L., Z.L., Z.H., D.W. and J.Y.. All authors have read and agreed to the published version of the manuscript.

**Funding**
This research was funded by the National Natural Science Foundation of China (Grant No. 82202907, 82373174, 82203301, 82203230), the Guangdong Basic and Applied Basic Research Foundation (Grant No. 2021A1515111157) and the Science and Technology Projects in Guangzhou (Grant No. 2023A04J1761, 2023A04J2145).

**Data availability**
Data is provided within the manuscript or supplementary information files.

## Declarations

**Ethics approval and consent to participate**
All animal experiments were proved by the ethics committee of Sun Yat-sen University (approval No. L025503202205014).

**Consent for publication**
Not applicable.

**Competing interests**
The authors declare no competing interests.

Received: 10 November 2024 Accepted: 20 February 2025
Published online: 06 March 2025

**References**

1. Shao J, Gao Y. Current cancer drug development strategies. Curr Cancer Drug Targets. 2019;19(4):243–4.
2. Wilcock P, Webster RM. The breast cancer drug market. Nat Rev Drug Discov. 2021;20(5):339–40.
3. Barnash KD, James LI, Frye SV. Target class drug discovery. Nat Chem Biol. 2017;13(10):1053–6.
4. Muttenthaler M, King GF, Adams DJ, Alewood PF. Trends in peptide drug discovery. Nat Rev Drug Discov. 2021;20(4):309–25.
5. Gratton JP, Yu J, Griffith JW, Babbitt RW, Scotland RS, Hickey R, Giordano FJ, Sessa WC. Cell-permeable peptides improve cellular uptake and therapeutic gene delivery of replication-deficient viruses in cells and in vivo. Nat Med. 2003;9(3):357–62.
6. Vives E, Schmidt J, Pelegrin A. Cell-penetrating and cell-targeting peptides in drug delivery. Biochim Biophys Acta. 2008;1786(2):126–38.
7. Wang L, Wang N, Zhang W, Cheng X, Yan Z, Shao G, Wang X, Wang R, Fu C. Therapeutic peptides: current applications and future directions. Signal Transduct Target Ther. 2022;7(1):48.
8. Rekdal O, Haug BE, Kalaaji M, Hunter HN, Lindin I, Israelsson I, Solstad T, Yang N, Brandl M, Mantzilas D, et al. Relative spatial positions of tryptophan and cationic residues in helical membrane-active peptides determine their cytotoxicity. J Biol Chem. 2012;287(1):233–44.
9. Branco MC, Sigano DM, Schneider JP. Materials from peptide assembly: towards the treatment of cancer and transmittable disease. Curr Opin Chem Biol. 2011;15(3):427–34.
10. Kuang Y, Long MJ, Zhou J, Shi J, Gao Y, Xu C, Hedstrom L, Xu B. Prion-like nanofibrils of small molecules (PriSM) selectively inhibit cancer cells by impeding cytoskeleton dynamics. J Biol Chem. 2014;289(42):29208–18.
11. Wang XJ, Cheng J, Zhang LY, Zhang JG. Self-assembling peptides-based nano-cargos for targeted chemotherapy and immunotherapy of tumors: recent developments, challenges, and future perspectives. Drug Deliv. 2022;29(1):1184–200.
12. Chen J, Wang W, Wang Y, Yuan X, He C, Pei P, Su S, Zhao W, Luo SZ, Chen L. Self-assembling branched amphiphilic peptides for targeted delivery of small molecule anticancer drugs. Eur J Pharm Biopharm. 2022;179:137–46.
13. Liu C, Somasundaram A, Manne S, Gocher AM, Szymczak-Workman AL, Vignali KM, Scott EN, Normolle DP, John Wherry E, Lipson EJ, et al. Neuropilin-1 is a T cell memory checkpoint limiting long-term antitumor immunity. Nat Immunol. 2020;21(9):1010–21.
14. Zhang J, Qiu J, Zhou W, Cao J, Hu X, Mi W, Su B, He B, Qiu J, Shen L. Neuropilin-1 mediates lung tissue-specific control of ILC2 function in type 2 immunity. Nat Immunol. 2022;23(2):237–50.
15. Wang S, Zhao L, Zhang X, Zhang J, Shang H, Liang G: Neuropilin-1, a myeloid cell-specific protein, is an inhibitor of HIV-1 infectivity. Proc Natl Acad Sci U S A 2022, 119(2).
16. Feng GK, Liu RB, Zhang MQ, Ye XX, Zhong Q, Xia YF, Li MZ, Wang J, Song EW, Zhang X, et al. SPECT and near-infrared fluorescence imaging of breast cancer with a neuropilin-1-targeting peptide. J Control Release. 2014;192:236–42.
17. Teesalu T, Sugahara KN, Kotamraju VR, Ruoslahti E. C-end rule peptides mediate neuropilin-1-dependent cell, vascular, and tissue penetration. Proc Natl Acad Sci U S A. 2009;106(38):16157–62.
18. Qin S, Liu Q, Li K, Qiu L, Xie M, Lin J. Neuropilin 1-targeted near-infrared fluorescence probes for tumor diagnosis. Bioorg Med Chem Lett. 2023;84:129196.
19. Ellerby HM, Arap W, Ellerby LM, Kain R, Andrusiak R, Rio GD, Krajewski S, Lombardo CR, Rao R, Ruoslahti E, et al. Anti-cancer activity of targeted pro-apoptotic peptides. Nat Med. 1999;5(9):1032–8.
20. Li X, Wang Y, Wang S, Liang C, Pu G, Chen Y, Wang L, Xu H, Shi Y, Yang Z. A strong CD8(+) T cell-stimulating supramolecular hydrogel. Nanoscale. 2020;12(3):2111–7.
21. Luo Z, Wu Q, Yang C, Wang H, He T, Wang Y, Wang Z, Chen H, Li X, Gong C et al: A Powerful CD8(+) T-Cell Stimulating D-Tetra-Peptide Hydrogel as a Very Promising Vaccine Adjuvant. Adv Mater 2017, 29(5).
22. Tao K, Levin A, Adler-Abramovich L, Gazit E. Fmoc-modified amino acids and short peptides: simple bio-inspired building blocks for the fabrication of functional materials. Chem Soc Rev. 2016;45(14):3935–53.
23. Liu Q, Cai S, Ye J, Xie Q, Liu R, Qiu L, Lin J: Preclinical evaluation of (68) Ga-labeled peptide CK2 for PET imaging of NRP-1 expression in vivo. Eur J Nucl Med Mol Imaging 2024.
24. Wang Q, Wang Y, Ding J, Wang C, Zhou X, Gao W, Huang H, Shao F, Liu Z. A bioorthogonal system reveals antitumour immune function of pyroptosis. Nature. 2020;579(7799):421–6.
25. Zhang Z, Zhang Y, Xia S, Kong Q, Li S, Liu X, Junqueira C, Meza-Sosa KF, Mok TMY, Ansara J, et al. Gasdermin E suppresses tumour growth by activating anti-tumour immunity. Nature. 2020;579(7799):415–20.
26. Wang Z, Meng F, Zhong Z. Emerging targeted drug delivery strategies toward ovarian cancer. Adv Drug Deliv Rev. 2021;178:113969.
27. Nussinov R, Tsai CJ, Jang H. Anticancer drug resistance: An update and perspective. Drug Resist Updat. 2021;59:100796.
28. Attwood MM, Fabbro D, Sokolov AV, Knapp S, Schioth HB. Trends in kinase drug discovery: targets, indications and inhibitor design. Nat Rev Drug Discov. 2021;20(11):839–61.
29. Acharya N, Anderson AC. NRP1 cripples immunological memory. Nat Immunol. 2020;21(9):972–3.
30. Liu X, Meng X, Peng X, Yao Q, Zhu F, Ding Z, Sun H, Liu X, Li D, Lu Y, et al. Impaired AGO2/miR-185-3p/NRP1 axis promotes colorectal cancer metastasis. Cell Death Dis. 2021;12(4):390.
31. Lin J, Zhang Y, Wu J, Li L, Chen N, Ni P, Song L, Liu X. Neuropilin 1 (NRP1) is a novel tumor marker in hepatocellular carcinoma. Clin Chim Acta. 2018;485:158–65.

32. Fu R, Du W, Ding Z, Wang Y, Li Y, Zhu J, Zeng Y, Zheng Y, Liu Z, Huang JA. HIF-1alpha promoted vasculogenic mimicry formation in lung adenocarcinoma through NRP1 upregulation in the hypoxic tumor microenvironment. Cell Death Dis. 2021;12(4):394.
33. Bao R, Surriga O, Olson DJ, Allred JB, Strand CA, Zha Y, Carll T, Labadie BW, Bastos BR, Butler M, et al. Transcriptional analysis of metastatic uveal melanoma survival nominates NRP1 as a therapeutic target. Melanoma Res. 2021;31(1):27–37.
34. Albanese A, Tang PS, Chan WC. The effect of nanoparticle size, shape, and surface chemistry on biological systems. Annu Rev Biomed Eng. 2012;14:1–16.
35. Barbir R, Capjak I, Crnkovic T, Debeljak Z, Domazet Jurasin D, Curlin M, Sinko G, Weitner T, Vinkovic Vrcek I. Interaction of silver nanoparticles with plasma transport proteins: A systematic study on impacts of particle size, shape and surface functionalization. Chem Biol Interact. 2021;335:109364.

## Publisher's Note